Frédéric Pascon, Guilhem Blès, Chantal Bouffioux, Silvia Casotto, Stefania Bruschi and Anne Marie Habraken:

Prediction of distortion during cooling of steel rolled rings using thermal-mechanical-metallurgical finite element model

Abstract: This work takes place in the framework of a CRAFT European project gathering three universities, three companies who produce rings through the ring rolling process and a manufacturer of temperature and dimension measurement devices. The final goal of the project is to develop and set up a system, integrated in the industrial process, capable of predicting the geometrical characteristics of final pieces just after the ring rolling stage and to allow the rolling process to avoid dimensional defects through online adaption. In fact, ring rolling production does not imply only the rolling process, but also the cooling and quench stages of steel rings. During all these phases, the dimensions of the pieces change dramatically. In particular, due to the lack of symmetry in the cooling conditions, ring distortions include contraction and rotation of the ring section. The modeling of the cooling phase requires taking into account a large number of phenomena resulting from the coupling of thermal, mechanical and metallurgical effects. A numerical model has been implemented in the non-linear finite element code LAGAMINE, developed by the University of Liège. Such a model can help to better understand the evolution of the geometry during the cooling phase and also the effects of each physical and microstructural parameter implemented in the model on the ring final shape. Effectively, several parameters can affect the ring distortions and the model should take them into account; in particular, the mechanical and thermal behavior of each phase present in the material (metastable austenite, ferrite, pearlite, bainite and martensite). Phase transformation modeling implies the integration of a wide data base of material properties (thermo-physical and mechanical properties of the phases, TTT and CCT diagrams, enthalpy and strain of phase transformation, strain of transformation plasticity…) but only a few of these data are available in literature. Some of them have been found for the reference material (42CrMo4 steel), but additional laboratory experiments have been performed at the Universities of Padua and Liège in order to characterize thermal, mechanical and plastic behaviour of phases. Finally, this paper presents the model validation on an industrial case (measurements of temperature and dimensions of rings have been provided by the manufacturer). Then, some applications are presented, demonstrating the importance of some factors such as some material properties, the shape of the rings, the type of cooling (and the cooling rate) or the symmetry of the cooling scheme on final ring distortion.

The ring rolling process is used to manufacture annular seamless parts from a bulk pierced billet through a complex sequence of axial-radial rolling operations carried out in hot and warm working conditions. Rolled rings are usually critical structural components utilized in assemblies of most strategic industrial sectors such as automotive and transportation, machine tools, food and chemical, energy, aircraft and aerospace.

The control of the geometry of the ring both during rolling and after final cooling to room temperature represents the main technological and economical limitation of the current technology.

In the framework of a CRAFT European project, an innovative modular system has been developed with the twofold objectives:

- on-line and real-time monitoring and control of all geometrical characteristics of rings just after hot and warm rolling operations;
- prediction of the geometry of the rings at the end of the cooling stage to room temperature.

Significant enhancement of capability and economy of the process as well as quality and reliability of the product are the main technological achievements expected from the project.

The paper presents the development of a suitably calibrated numerical model capable of predicting ring distortion during the cooling phase after ring rolling operations.

A 2D axi-symmetric model has been set up, using the LAGAMINE finite element code, which has been developed at University of Liege since the early nineteen-eighties. This model includes thermal and mechanical aspects as well as phase transformations. The next section describes more detail of this model.

Due to difficulties in characterizing the material properties, to date we focus only on one material. The material studied is a 42CrMo4 steel, which is commonly used in ring production. Its chemical composition is given in **Table 1**.

Table 1: Chemical composition of 42CrMo4 steel (ref: producer of studied rings)

C	Mn	Si	Cr	Mo
0.42%	0.80%	0.30%	1.00%	0.25%

Most of the material properties introduced in the model are from a large literature review on 42CrMo4 and similar steels. Some others have been determined experimentally.

Description of the numerical model

The numerical model has to be able to predict the ring distortion due to cooling (after ring rolling) from elevated temperatures and to take into account all the phenomena

PhD Frederic Pascon; PhD Guilhem Blès; Chantal Bouffioux, Mechanics & Structures Department, Université de Liège – Belgium; *Silvia Casotto; PhD Stefania Bruschi,* Dipartimento di Innovazione Meccanica e Gestionale, Università degli Studi di Padova – Italy ; *PhD Anne Marie Habraken,* Mechanics & Structures Department, Université de Liège – Belgium

leading to the final geometry. In particular, geometrical distortion can be modelled only if the non-simultaneous and non-symmetric cooling conditions are included in the model. In other respects, phase transformations must also be taken into account.

The numerical model presented in this paper has been implemented in the LAGAMINE finite element code [1].

Phase transformation model. During cooling, steel rings undergo several phase transformations, which occur at different temperatures and times according to several parameters, among others steel grade and cooling rate.

Transformations by diffusion. These transformations are based on two microscopic phenomena: germination of particles and their growth. Extending models of isothermal transformations to continuous cooling, we use an „additivity principle"; the final microstructure is the result of a succession of elementary isothermal transformations, each one being independent on thermal history. The consequence is the possibility of using TTT diagrams instead of CCT diagrams, which cannot exactly reproduce thermal history for any ring (different shapes, cooling conditions, etc.).
The germination is achieved when Scheil's sum reaches unity:

$$\int_0^{t_j} \frac{dt}{\Pi} \cong \sum_{i=1}^{j} \frac{\Delta t_i}{\Pi(T_i)} = 1 \qquad (1)$$

where $\Pi(T)$ is germination time for an isothermal transformation at temperature T and t_j is germination time for continuous cooling $T(t)$. The cooling curve is modelled by successive isothermal steps Δt_i at constant temperature T_i.
Johnson-Mehl-Avrami law is then used for growth modelling [2]:

$$y_k = 1 - exp\left(-b_k t^{n_k}\right) \qquad (2)$$

where y_k is the volume fraction of phase k (austenite, ferrite, pearlite, bainite), b_k and n_k are temperature dependent parameters of phase k and t is time counted from germination.

The model integrates a TTT-diagram of 42CrMo4 steel coming from the literature review and pictured on Fig 1 [3].

Martensitic transformation. The martensite proportion during cooling is governed by Koistinen-Marburger law:

$$y_{Ma}(T) = 1 - exp\left(-\alpha_{Ma}\left(M_s - T\right)\right) \qquad (3)$$

which only depends on temperature T. The constants M_s (martensitic temperature) and α_{Ma} are respectively equal to 331 °C and 0.011 K^{-1} as found in literature [4].

Thermal model. The thermal model includes both internal conduction (in the ring) and heat extraction from the ring to its surroundings. These rates of heat transfer **q** are characterized by thermal conductivity k and heat transfer coefficients h_{tc}:

$$\begin{cases} \boldsymbol{q} = -k\nabla T & \text{in } \Omega \text{ (the ring)} \\ \boldsymbol{q} = h_{tc}\left(T_s - T_\infty\right)\boldsymbol{n} & \text{on } \Sigma \text{ (the surface)} \end{cases} \qquad (4)$$

The differential equation describing heat balance is the classical Fourier law:

$$\rho c\dot{T} + \nabla \cdot \boldsymbol{q} = \dot{Q} \qquad (5)$$

where ρ is the density, c the specific heat and Q the heat generation/extraction, in this case represented by enthalpy of phase transformation and/or heat exchange (at the surface of the ring).

These material properties (k, ρ, c, $\dot{Q}$) are characteristics of each phase and temperature dependent. Equivalent values x_{eq} are therefore computed according to a mixture law and then used in the heat balance (5):

$$x_{eq}(T, y_k) = \sum_{k=1}^{5} y_k x_k(T) \qquad (6)$$

where the sum integrates the contribution of the 5 possible phases (austenite, ferrite, pearlite, bainite, martensite).

Heat transfer coefficients include both convection and radiation terms:

$$h_{tc}(T) = h_{conv} + \varepsilon_r \sigma_{SB}\left(T_s + T_\infty\right)\left(T_s^2 + T_\infty^2\right) \qquad (7)$$

where h_{conv} is the convection term, ε_r the relative emissivity and σ_{SB} the Stefan-Bolzmann constant.

Mechanical model. The mechanical analysis involves the determination of the stresses and strains due to ring cooling. The model is based on the decomposition of the total strain rate tensor $\dot{\varepsilon}$ into several contributions:

$$\dot{\varepsilon}_{ij} = \dot{\varepsilon}_{ij}^{el} + \dot{\varepsilon}_{ij}^{pl} + \dot{\varepsilon}_{ij}^{th} + \dot{\varepsilon}_{ij}^{tr} + \dot{\varepsilon}_{ij}^{pt} \qquad (8)$$

where the five terms are respectively elastic, plastic, thermal, transformation and transformation plasticity strain rates.

Thermal strain rate is assumed to be hydrostatic and its value for each phase is directly linked to temperature rate $\dot{T}$ through the thermal linear expansion coefficient α:

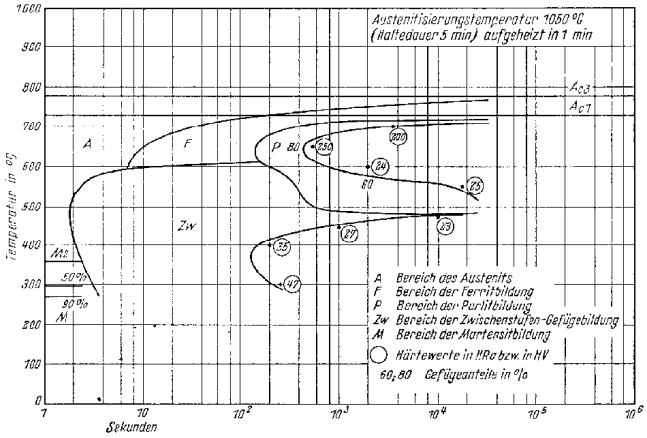

Fig 1: TTT-diagram of 42CrMo4 steel [3]

$$\dot{\varepsilon}_m^{th} = \sum_{k=1}^{5} \left(y_k \alpha_k (T) \dot{T} + \dot{y}_k \int_0^T \alpha_k (\theta) d\theta \right) \qquad (9)$$

Experimental curves of dilatation allow the determination of such α_k coefficients for each phase.

Phase transformations are accompanied by a change in volume (leading to transformation strain rate $\dot{\varepsilon}_{ij}^{tr}$, which is purely volumetric) and a pseudo-plasticity effect commonly known as the transformation plasticity $\dot{\varepsilon}_{ij}^{pt}$ (see **Fig 2-3**).

The integration of the stress tensor is classically based on a plasticity flow rule associated to von Mises' yield surface with isotropic hardening. A bi-linear elastoplastic constitutive law has been assumed, although an elastoviscoplastic law could be [2]. Material properties are then fit to match the stress level corresponding to strain rates compatible with the problem and the possibilities of experimental devices (Gleeble 3800 thermo-mechanical simulator).

Material properties – Young's modulus $E(k,T)$, Poisson's coefficient $\nu(k,T)$, yield limit $\sigma_y(k,T)$ and tangent modulus $E_t(k,T)$ – are characteristics of each phase k and temperature dependent. In the model, equivalent values based on relation (6) are computed according to actual configuration.

Effect of stress on phase transformations. The model takes into account the effect of stress level on the kinetics of phase transformations [4] responsible of the shift of TTT-diagram:

$$\begin{cases} D(\sigma) = C\bar{\sigma} \\ t_{begin}(\sigma) = (1-D)\, t_{begin}(\sigma = 0) \\ b(\sigma) = (1-D)^{-n}\, b(\sigma = 0) \end{cases} \qquad (10)$$

where C is a constant, t_{begin} is the time at the beginning of the phase transformation, n and b are the coefficients of the Johnson-Mehl-Avrami law (2).

In other respects, the stress level also influences the martensitic transformation:

$$M_s = M_{s,\sigma=0} + A\sigma_m + B\bar{\sigma} \qquad (11)$$

In the model, the C constant in relation (10) is assumed to be equal to 8.5 10^{-3} MPa^{-1} (obtained during an isothermal transformation at 663°C), while A is 0.05 K/MPa and B is 0.033 K/MPa. These values are coming from [4] for XC80 steel, since we had no value for 42CrMo4.

Initial conditions. The model is applied to the cooling of the rings after rolling. Our initial conditions therefore correspond to the end of the rolling stage, which could be obtained by means of 3D F.E. models (such as those first developed by Kim et al., Hu et al. and Lim et al. [6-9], or more recently by Davey and Ward [10]).

However, such 3D models require much time (CPU as well as in the development of the model itself). Moreover, the aim of our model is to predict the effect of different factors (geometry and size of the ring, coolant, etc.) on the ring distortion during cooling (after rolling).

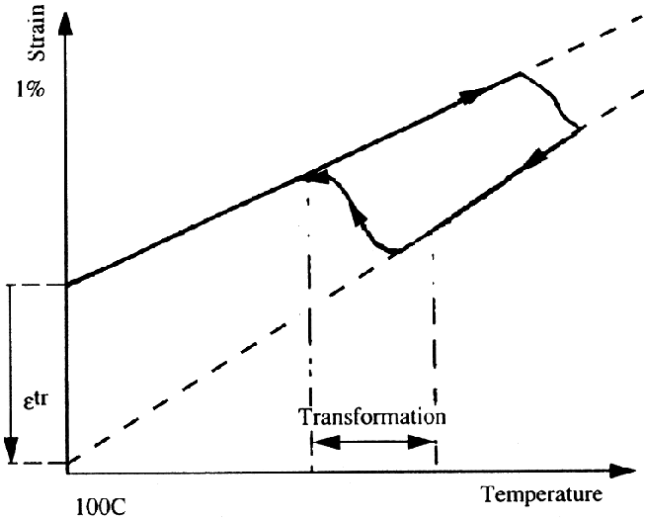

Fig 2: Volumetric strain due to phase transformation ε_{ij}^{tr}

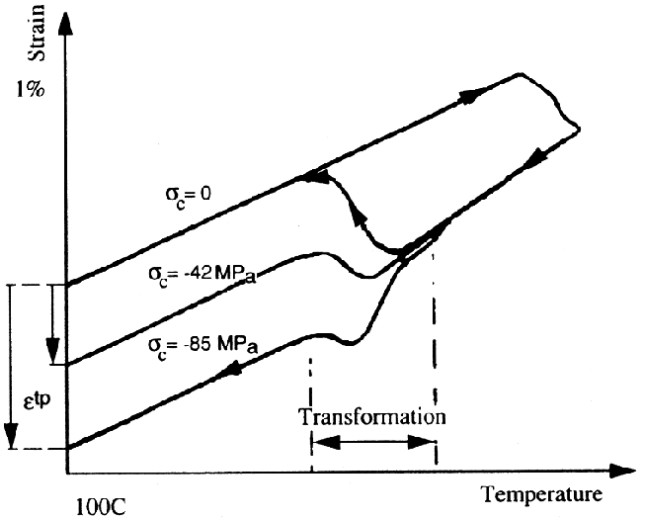

Fig 3: Pseudo-plasticity effect or transformation plasticity ε_{ij}^{pt} [5]

We have thus decided to adopt the following assumptions:

- nominal rectangular geometry and nominal dimensions;
- neither initial stress nor initial strain;
- the initial temperature field corresponding to a „pre-cooling" of the ring in the air from 1080°C (uniform temperature in the ring) down to a mean surface temperature equal to 880°C (as measured on the production line) – see **Fig 4**.

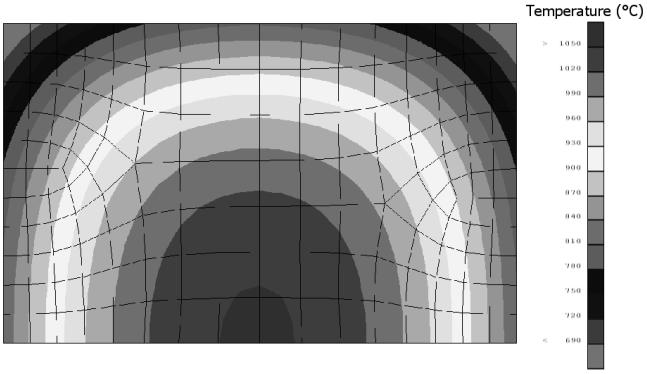

Fig 4: Initial temperature field obtained after an air cooling from 1080°C to 880°C

Validation of the numerical model

Simulation of the process. Some measurements have been carried out on 5 rings directly in the production line. These measurements have been used to validate the model.

At the rolling stage, the dimensions of the measured rings have been assumed to be the nominal ones, i.e.

$$D_i = 1085 \text{ mm} \quad D_e = 1197 \text{ mm} \quad H = 85 \text{ mm} \qquad (12)$$

without any planarity or taper defects.

The geometry and surface temperature of the rings are then measured by means of a laser device 180s after the end of rolling (see **Fig 5**).

This operation is repeated after the complete cooling of the rings, i.e. at room temperature, together with a manual measurement, allowing the validation of the laser-beam measurement.

Simulation of the process. The rings have been modelled from the end of the ring rolling until the complete cooling. It has been performed in two steps: the first step corresponds to the cooling from rolling stage to the first laser-beam measurement and the second one is the successive cooling down to room temperature.

Simulation of the first step of the process. The simulation of this first step requires the knowledge of the cooling starting conditions in terms of dimensions and temperature distribution in the ring section.

The key problem is the lack of information about the temperature distribution inside the ring, since the only available measurement is surface temperature. We assumed the process, during the first step, to be equivalent to the following scheme and assumptions:

- uniform initial temperature in the ring (T_0 = 1080°C, i.e. temperature just after rolling, measured by optical pyrometer)
- initial geometry = nominal rolling geometry – cf. (12)
- effective heat transfer coefficients on the 4 faces of the ring that reproduce the heat transfer due to real manipulations of the ring (rolling and transfer during 180s on a conveyor to the laser-beam measurement site)
- consider the cooling of the ring during an equivalent time (not necessarily 180s) that leads to a final geometry and a surface temperature of the ring at the end of this first step that correspond to the measurements

After having checked that the geometry and surface temperature predicted by the model under these conditions correspond to the actual laser-beam measurements, it can be assumed that the unknown temperature distribution inside the ring should correspond to the real one.

Second step of the process. Now, considering an initial temperature distribution and an initial geometry corresponding to the end of the first step, we applied heat transfer coefficients corresponding to the real situation (air cooling). When the ring is at room temperature, its geometry is checked and compared to the second set of measurements.

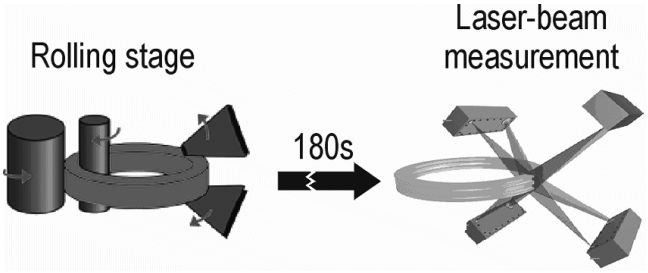

Fig 5: Laser-beam system for measurement of ring's dimensions (180s after rolling stage and after complete cooling)

Fig 6 shows the evolution of internal and external diameters during the process (at rolling stage, at the first measurement and at room temperature). The difference between simulations and average measurements is less than the standard deviation of the 5 samples set.

Sensitivity analyses

Sensitivity to material properties. Sensitivity analyses have been performed to clearly identify the key parameters for numerical simulations. Such analyses have been focused on:

- material properties
- heat transfer coefficients
- ring position in the pile after the cooling stage

Results of these analyses allow focussing the attention only on parameters critical for the setting up of the model.

Influence of material properties. This first sensitivity analysis has been performed to identify which phase properties must be known with high accuracy.

To determine the parameters having the greatest impact on the ring distortion, each material property has been perturbed (one at time) by +20%; then the results in terms of final geometry have been compared to the reference case.

Average impact I. To evaluate the impact of the different properties on ring distortion, the following geometrical characteristics have been analysed (see **Fig 7**):

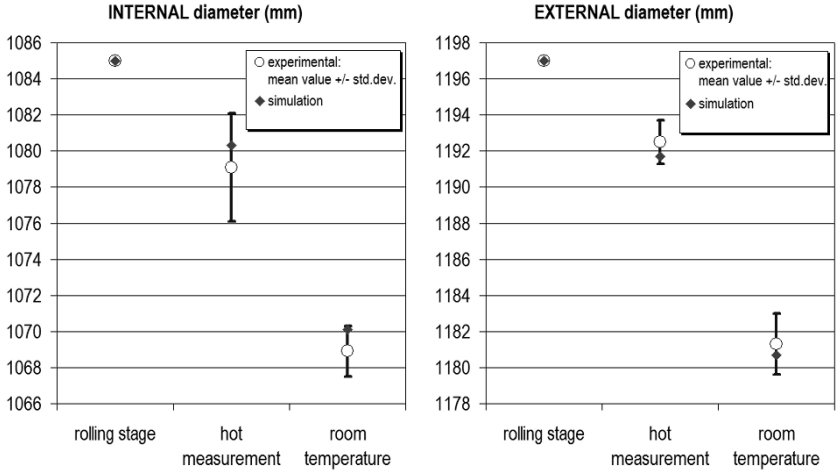

Fig 6: Evolution of internal and external diameters

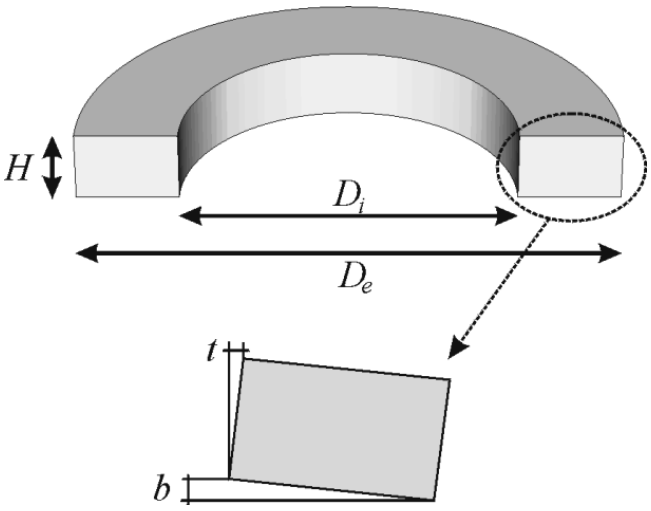

Fig 7: Geometrical characteristics of distorted rings

- internal and external diameters D_i and D_e
- height H
- planarity b
- taper t

After the complete cooling, these five characteristics have been compared to the initial ones (just after the rolling stage), characterising the ring distortion by:

- variations in diameters ΔD_i and ΔD_e
- variation in height ?H

while planarity b and taper t are direct measures of the distortion (it has been assumed that, at the end of the ring rolling, the ring has nominal rectangular geometry and nominal dimensions).

When one material property is perturbed, distortion is characterized by variations in diameters $\Delta' D_i$ and $\Delta' D_e$, variation in height H', planarity b' and taper t'.

When these values are rather similar to the reference ones, the perturbed property is not considered as a key parameter since a 20% lack of accuracy of its value would not significantly affect the final distortion. **Fig 8** shows the average impact of most material properties on ring distortion. This average impact factor I is given by:

$$I = \frac{1}{5}\left(\frac{\Delta D'_i - \Delta D_i}{\Delta D_i} + \frac{\Delta D'_e - \Delta D_e}{\Delta D_e} + \frac{\Delta H' - \Delta H}{\Delta H} + \frac{b' - b}{b} + \frac{t' - t}{t} \right) \quad (13)$$

A first remark concerns the properties of martensite phase; in this sensitivity analysis, we assumed air cooling. In such a case, the cooling rate is quite low (with respect to quench in water for example). Martensite does not appear in such a case and its properties obviously do not affect the ring distortion.

From the above results, three different kinds of behaviour can be pointed out:

- A very large impact is predicted for a 20% perturbation of the T.L.E. coefficients α, especially for austenite (Au), ferrite (Fe) and pearlite (Pe) phases (I > 6%), in a lesser way for bainite (Ba) phase (I > 2%).
- A medium impact is predicted for different properties, leading to an average impact between 0.5% and 2%. This is the case for a 20% perturbation of:
- thermal conductivity of Au, Fe and Pe phase;
- specific heat of Au phase;
- strain of phase transformation for Au→Fe and Au→Ba transformations;
- strain due to transformation plasticity for Au→Fe and Au→Pe transformations;
- yield limit of Au, Fe and Pe phases.
- A low impact (I < 0.5%) or (almost) no impact for 20% perturbations of other material properties, especially for elastic properties (Young's modulus and Poisson's coefficient), tangent modulus, enthalpy of phase transformation and coefficient of TTT-diagram shifting.

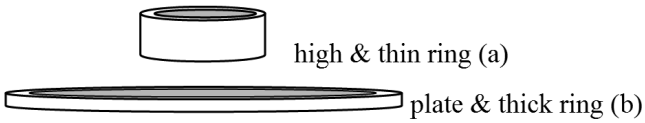

Fig 9: Comparison of two shapes of ring

Influence of the shape of the ring. We studied the effect of the shape of the ring on its distortion. Here is an example comparing two types of ring (**see Fig 9**), the first one being relatively high, but thin and the second one being thicker, but rather plate-like.

In that case, the rings are quenched in a water and polymer solution, allowing much faster cooling than in the previous case (cooling in the air).

Figures 10-11-12 illustrate some results: The thick ring exhibits large distortion, including a rotation that does not occur in the case of the thin ring. In other respects, the bulk of the thin ring is much lower than that of the thick one; that entails a higher cooling rate and a higher proportion of bainite and martensite.

Influence of the cooling rate. This analysis consists of the comparison of the cooling of the same ring with different heat transfer coefficients. We consider here the plate and thick ring presented above (Fig 9.b). The ring is quenched in the same water + polymer solution considering

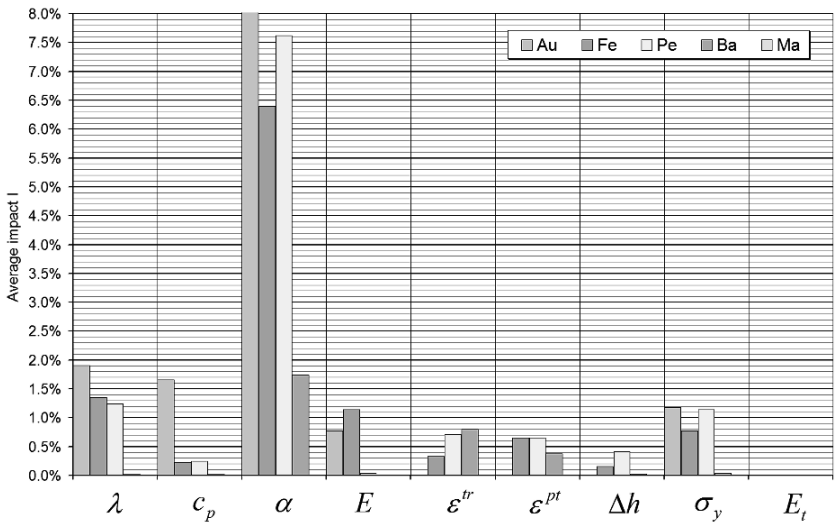

Fig 8: Average impact of most of the material properties on ring distortion

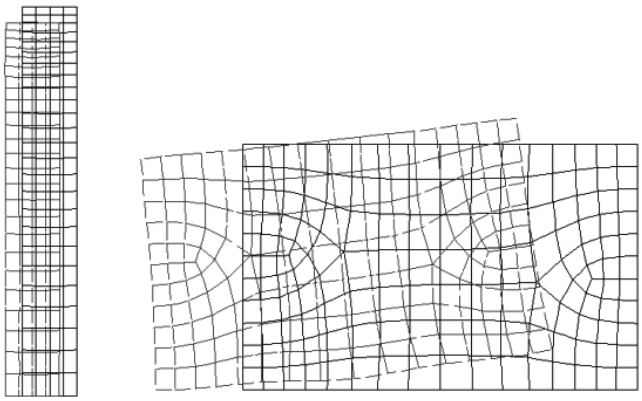

Fig 10: Distortion of the two studied rings (displacements are multiplied by 10)

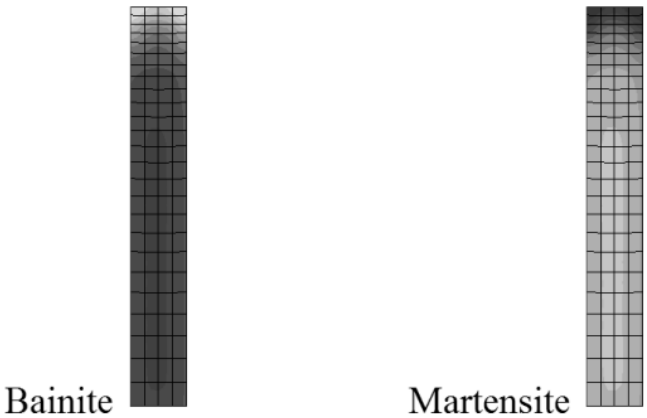

Fig 11: Phases distribution in the tall and thin ring (without neither ferrite nor pearlite formation)

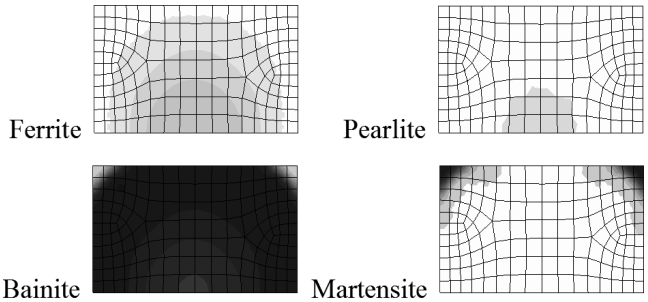

Fig 12: Phases distribution in the plate and thick ring

two velocities of the bath; in the first case agitators create flows in the bath at 0.5 m/s (h_{tc} identical to the previous section), in a second case 0.2 m/s. Heat transfer coefficients in both cases have been determined experimentally and – as expected – higher coefficients have been found for higher velocity.

Besides the difference in phase distribution, another significant and unexpected result concerns the ring distortion, mainly represented by section rotation. At higher velocity (0.5 m/s) the section rotates anticlockwise, while the rotation is clockwise when the heat transfer coefficient decreases with velocity (0.2 m/s) – see **Fig 13**.

Influence of the position of the ring during cooling. During production, rings are stacked in piles when introduced in the bath (water + polymer). According to the position of the ring in the stack and the way that the pile is mounted, the rings exhibit two, three or four faces to the bath. Rings may be piled up directly or using blocks between each ring, allowing fluid flow – and thus cooling – on the four faces.

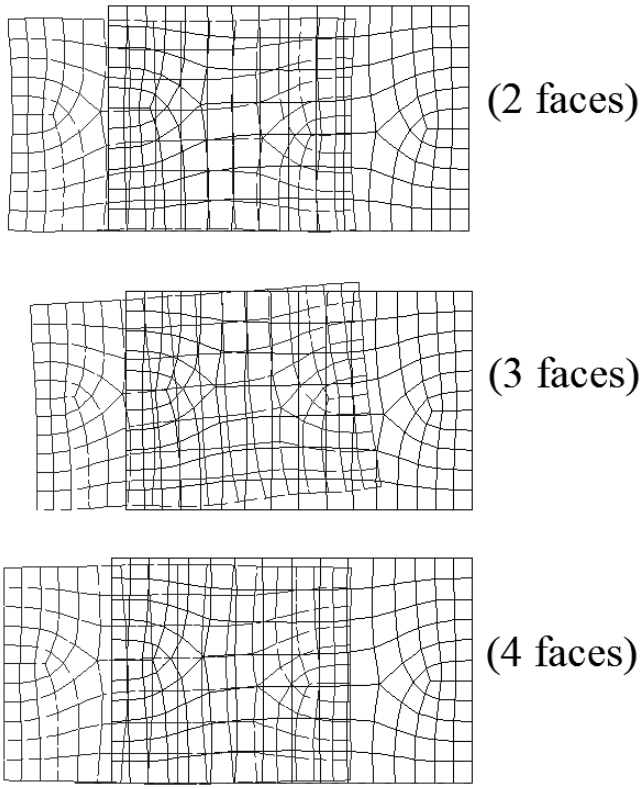

Fig 14: Distortion of the ring for 2-3-4 cooled faces (displacements are multiplied by 10)

Results for the plate & thick ring cooled in the air are presented considering the three following cases:

- 2 faces cooled (in the pile, without blocks)
- 3 faces cooled (top of the pile, without blocks)
- 4 faces cooled (anywhere in the pile, with blocks)

Fig 14 clearly shows that in the second case (3 faces – the most asymmetric one), distortion is accompanied with a rotation which does not appear in the other two cases. Another impact of these cooling schemes is represented by the residual stresses in the rings (see **Fig 15**).

Conclusions

A 2D axi-symmetric model based on the finite element method has been set up to model cooling of rolled rings. Some simplifying assumptions have been necessary to define initial conditions of the model (thermal and mechanical

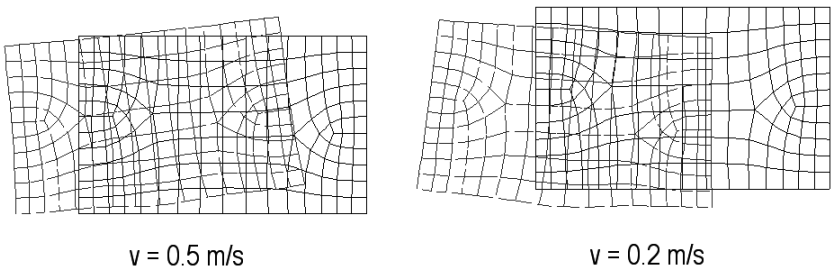

Fig 13: Distortion of the ring for two different cooling rates (displacements are multiplied by 10)

state of the ring at the end of the rolling stage). Different results on 42CrMo4 steel rings are presented and the effect of some parameters on the ring distortion has been pointed out:

- massive sections exhibit higher rotations;
- cooling rate can modify the direction of the rotation;
- non-symmetric cooling scheme is responsible for non-symmetric distortion (rotation).

Sensitivity analysis to properties of phases also allowed classification of the key parameters. This is a helpful tool to evaluate the accuracy and the need to perform experiments when data is not available in the literature.

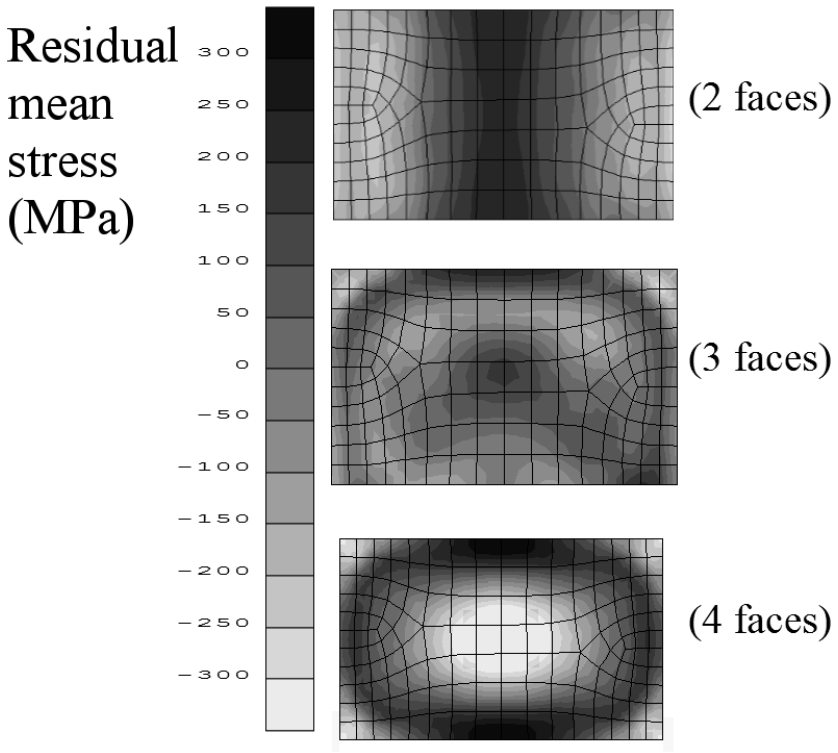

Fig 15: Residual mean stresses in the ring for 2-3-4 cooled faces

Acknowledgements

This cooperative research takes place in the Fifth Framework Program supported by the European Commission (project reference G1ST-CT-2002-50162). We express our gratitude to the industrial partners Tecnogamma (Italy), CFR (Arcelor Group, Belgium), Forgital (Italy) and Ovako Steel (SKF Group, Sweden). Parts of this paper are extracted from RW9813793 project supported by Walloon Region. As Research Associate of National Fund for Scientific Research (Belgium), A.M. Habraken thanks this Belgian research fund for its support.

References

[1] A.M. Habraken: Contribution à la modélisation du formage des métaux par la méthode des éléments finis, Université de Liège, 1989 (PhD. Thesis)

[2] A.M. Habraken, M. Bourdouxhe: Eur. J. Mech. A/Solids, Vol 11 (1992), n°3, p. 381/402

[3] F. Wever, A. Rose, W. Peter, W. Strassburg, L. Rademacher: Atlas zür Wärmebehandlung der Stälhe, Verlag Stalheisen M.B.H. – Düsseldorf, 1958

[4] S. Judlin-Denis: Modélisation des interactions contrainte – transformation de phase et calcul par éléments finis de la génère des contraintes internes au cours de la trempe des aciers, Inst. Nat. Polytechnique de Lorraine (France), 1987 (PhD. thesis).

[5] U. Chandra, A. Ahmed: Modelling for Casting and Solidification Processing – Chapter 3: Stress Analysis, ISBN 0-8247-8881-8, Kuang-O (Oscar) Yu Ed., Marcel Dekker, Inc. New York – Basel, 2002.

[6] N. Kim, S. Machida, S. Kobayashi: Int. J. Machine Tools Manufacturing, Vol. 30 (1990), n°4, p.569-577

[7] Z.M. Hu, I. Pillinger, P. Hartley, S. McKenzie, P.J. Spence in: Simulation of materials processing: theory and applications. S.F. Shen, P.R. Dawson editors, Balkema (Rotterdam), 1995, p. 941-946

[8] Z.M. Hu, I. Pillinger, P. Hartley, S. McKenzie, P.J. Spence: J. Materials Processing Technology, Vol. 45 (1994), p. 143-148

[9] T. Lim, I. Pillinger, P. Hartley: J. Materials Processing Technology, Vol. 80-81 (1998), p. 199-205

[10] K. Davey, M.J. Ward: Int. J. Mech. Sci., Vol. 44 (2002), p. 165-190